Heterogeneous dynamics and ageing in a dense ferro-glass

2008 J. Phys.: Condens. Matter 20 204124

(http://iopscience.iop.org/0953-8984/20/20/204124)

IOP PUBLISHING JOURNAL OF PHYSICS: CONDENSED MATTER

J. Phys.: Condens. Matter **20** (2008) 204124 (5pp) doi:10.1088/0953-8984/20/20/204124

Heterogeneous dynamics and ageing in a dense ferro-glass

E Wandersman[1], E Dubois[1], V Dupuis[1], A Duri[2], A Robert[3,4] and R Perzynski[1]

[1] Université Pierre et Marie Curie-Paris 6, Laboratoire Liquides Ioniques et Interfaces Chargées (UMR 7612 UPMC/CNRS/ESPCI), 4, place Jussieu,-case 51, 75252 Paris Cedex 05, France

[2] Deutsches Elektronen-Synchrotron (Hasylab), Notkestraße 85, 22607 Hamburg, Germany

[3] European Synchrotron Radiation Facility, 6 rue J Horowitz BP 220, 38043 Grenoble Cedex 9, France

[4] Linac Coherent Light Source, Stanford Linear Accelerator Center, Stanford University, LUSI/LCLS-2575 Sand Hill Road, MS 43A Menlo Park, CA 94025, USA

E-mail: wanders@ccr.jussieu.fr

Received 31 March 2008
Published 1 May 2008
Online at stacks.iop.org/JPhysCM/20/204124

Abstract

Repulsive magnetic fluids show a dynamical freezing above a volume fraction Φ^*, which depends on the physico-chemistry of the system. Φ^* is here determined by a magneto-optical technique. The out-of-equilibrium dynamics of a glass-forming magnetic fluid ($\Phi = 1.2\Phi^*$) is studied by x-ray photon correlation spectroscopy and analyzed in terms of intensity auto-correlation functions. The relaxation is age dependent and follows a compressed exponential law with a characteristic time scaling as the inverse of the scattering vector Q. The dynamical susceptibility χ is then deduced from a time resolved correlation analysis at an intermediate Q and for ages larger than 10^4 s.

(Some figures in this article are in colour only in the electronic version)

1. Introduction

In a wide class of disordered materials, the transition from the fluid to the solid phase leaves the system in an out-of-equilibrium configuration. This transition, driven by the density Φ, the temperature T or the stress Σ, takes place in granular matter or in colloidal systems and is characterized by a sudden dynamical arrest, occurring without any growth of structural static order. In the solid phase, particles are confined in a small region of the phase space from where they hardly escape. As a consequence, the term 'jamming transition' is usually employed and a jamming phase diagram proposed in the $(1/\Phi, T, \Sigma)$ plane [1, 2] is able to unify the results from granular and soft matter. However, the precise nature of the dynamical slowing down accompanying the jamming transition is still unclear.

In jammed soft matter, experimental and numerical investigations of slow dynamics are numerous, from the point of view of the positional degrees of freedom on the micron scale [3]. However only scarce results have been reported on the freezing of colloidal nanoparticles throughout the transition, probing both positional and orientational degrees of freedom. We will focus here on these last two points and on associated ageing processes inside aqueous ionic ferrofluids (i.e. electrostatically stabilized), which present at large volume fractions a fluid–solid transition. A physico-chemical control of the dispersion [4] allows us to tune the interparticle interaction. Moreover magneto-optical and scattering properties of the nanoparticles enable us to probe their orientational and translational degrees of freedom while the system is undergoing the glass transition [5, 6]. The aqueous dispersions of magnetic nanoparticles are prepared, thanks to an osmotic compression method. Well-defined states are obtained by tuning interparticle interactions and they can be localized inside a well-known region of the phase diagram, which is similar to that of molecular systems [4]. The experimental control parameters, determining the state of interaction of the dispersion, are the osmotic pressure and the ionic strength. At the end of the compression, the volume fraction resulting from the osmotic process is determined by

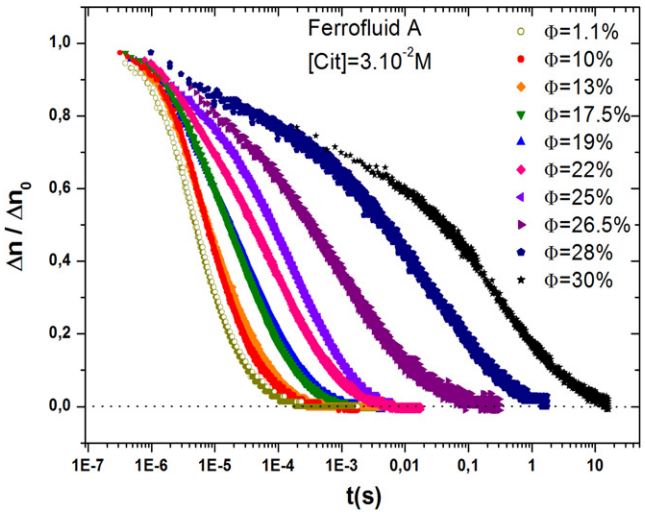

Figure 1. Relaxation of normalized birefringence $\Delta n/\Delta n_0$ for samples of increasing volume fraction Φ.

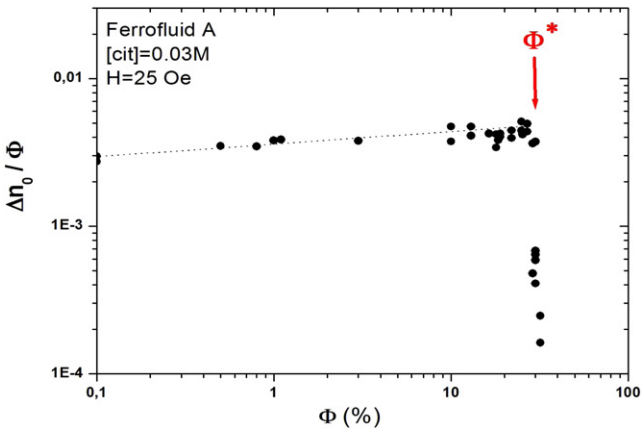

Figure 2. Maximum birefringence Δn_0, normalized by the volume fraction Φ of the dispersion, detected in the magneto-optical experiment with a pulsed magnetic field (2 kA m^{-1}, pulse duration 2 s) as a function of Φ.

chemical titration. We explore here the dynamical properties of strongly repulsive dispersions based on γ-Fe_2O_3 nanoparticles (of mean diameter $d \sim 10$ nm) stabilized by citrate species (Ferrofluid A, [cit] $= 3 \times 10^{-2}$ M). In these dispersions, the osmotic pressure is much larger than that of a perfect gas of equivalent nanoparticles [4]. The polydispersity of the dispersed nanoparticles avoids any crystallization at high volume fractions and fluid-like structures are observed, as evidenced by small-angle neutron scattering [5].

By using several experimental techniques, we have evidenced that a dynamical freezing is reached if the volume fraction of magnetic material is larger than a given value Φ^*. A freezing of the positional degrees of freedom is observed, by Rayleigh forced scattering [7] and by x-ray photon correlation spectroscopy (XPCS) [6], a freezing of the rotational dynamics being also evidenced in magneto-optical experiments [5].

2. Glass-forming ferrofluids—freezing of the rotational dynamics

A magneto-optical probing of the dispersions is possible because of the optical anisotropy of the particles (related to their magnetic moment $\vec{\mu}$). Under an applied field, the nanoparticles orient along the field direction and the whole dispersion acquires a macroscopic magnetization. It creates as well an optical birefringence as a result of the alignment of the optical axes of the nanoparticles [8]. By measuring the birefringence response to a pulse of magnetic field, we are able to probe the degree of mechanical orientation of the nanoparticles inside the medium [5, 9].

We explore here a wide range of volume fractions Φ, from dilute up to macroscopic solid samples. Figure 1 illustrates the volume fraction dependence of the birefringence relaxation $\Delta n(t)$, normalized at $t = 0$, after an applied pulse of field amplitude 2 kA m^{-1} and duration 2 s. For dilute samples, the birefringence $\Delta n_0 = \Delta n(t = 0)$ is proportional to Φ and the nearly exponential relaxation can be described in terms of Brownian rotational diffusion. The dynamics slow down with increasing volume fraction and spread over six decades from microseconds up to several seconds. The slowing down at large Φ is observed with a broadening of the characteristic time distribution as well as a turn over to a non-exponential shape of the relaxation [5]. Above a certain value Φ^*, the detected magneto-optical intensity drastically falls [5], expressing the freezing of the rotational dynamics, as illustrated in figure 2. We have shown in [5] that Φ^* depends both on the size of the nanoparticles and on the ionic strength of the dispersion. Φ^*, which corresponds to a volume fraction at which the particles are far from being in contact, is associated with the freezing of the rotation of effective spheres, constituted of the nanoparticles and of their surrounding ionic cloud. Thus, for volume fractions $\Phi > \Phi^*$, the effective spheres interpenetrate and the system is becoming glass forming with a widely spread distribution of characteristic times. The (rather low) birefringence signal increases logarithmically with $T_{\rm pulse}$, the relaxation becoming even slower as $T_{\rm pulse}$ is increasing. Moreover, an ageing of the system is also observed in these glass-forming dispersions [10]. For concentrated dispersions, general dynamical features of the glass transition are thus observed for the degrees of freedom of mechanical orientation.

3. X-ray photon correlation spectroscopy experiments—translational ageing

It is also possible to study the translational dynamics of such colloidal dispersions by x-ray photon correlation spectroscopy. However the experimental accessibility in terms of intensity and relaxation time is rather narrow, while probing dispersions of nanoparticles. It is nevertheless possible to explore the ergodic–non-ergodic properties of such a glass-forming system at $\Phi/\Phi^* \sim 1.2$ using XPCS and to probe the out-of-equilibrium translational dynamics of the dispersions [6]. The XPCS experiment is carried out at the ID10C branch of the TROIKA beam line at the European Synchrotron Radiation Facility (ESRF). Figure 3(a) gives a typical speckle pattern

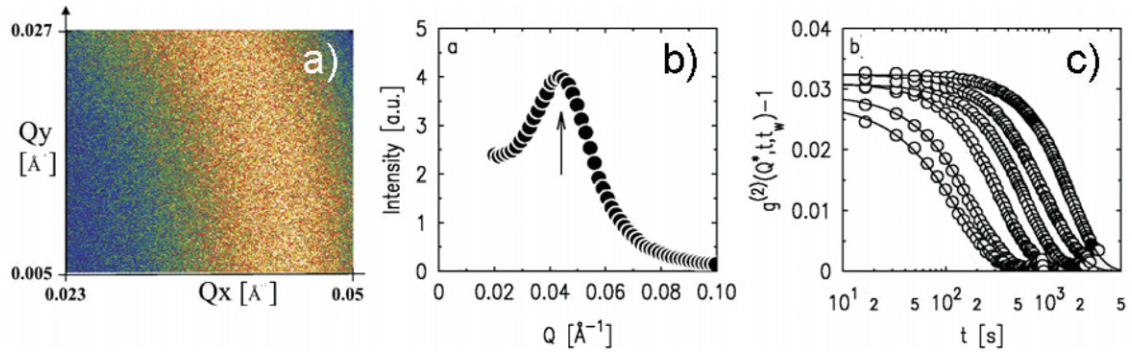

Figure 3. Results of XPCS experiments for a glass-forming sample ($\phi = 30\%$; nanoparticles with a log-normal distribution of magnetic diameters: $d_0 = 9.5$ nm, $\sigma = 0.35$). (a) Two-dimensional speckle pattern. (b) Static scattered intensity as a function of scattering vector Q. The arrow indicates the maximum of intensity, at the scattering vector Q^*. (c) Second-order correlation function at $Q^* = 0.044$ Å^{-1} and $t_W = 1400$ to 13 100 s, increasing from left to right. Solid lines are best fits of the data using equation (2).

obtained from an XPCS experiment as recorded by a charge coupled device (CCD) camera. Qx and Qy are the horizontal and vertical components of the scattering vector Q. It shows a section of the annulus associated with the expected static correlation ring. The small-angle scattering intensity of the sample, which is given in figure 3(b) as a function of Q, does indeed present a static correlation peak (corresponding to the annulus of figure 3(a)) at an intermediate scattering vector $Q^* = 0.044$ Å^{-1}. It corresponds to the most probable interparticle distance of 14 nm. Such an intensity profile is typical of a glass-forming ferrofluid with repulsive interactions. The decrease of intensity at low Q results from the low macroscopic compressibility of this repulsive system (here of the order of 0.05).

To probe the dynamics, long-time series of speckle patterns are recorded while the sample ages (over typically 10–12 h). In order to determine the ensemble-averaged intensity autocorrelation function at a certain age t_W, we evaluate the second-order correlation function [11]

$$g^{(2)}(Q,\tau,t_W)-1 = \frac{\langle I_p(Q,t_W)I_p(Q,t_W+\tau)\rangle_Q}{\langle I_p(Q,t_W)\rangle_Q \langle I_p(Q,t_W+\tau)\rangle_Q} - 1 \quad (1)$$

where I_p is the scattered intensity at the pixel p of the CCD camera and $\langle\cdots\rangle_Q$ denotes the circular average over a ring of pixels corresponding to scattering vectors Q of the same amplitude and different azimuthal directions. To calculate $(g^{(2)}(Q,\tau,t_W)-1)$ as a function of the lag time τ, a time average over a series of frames centered around time $t = t_W$ (within the time window $T_{\rm exp}$) is performed. The ensemble average (required for glass-forming samples presenting non-ergodic features) is thus realized. Age initialization $t_W = 0$ is defined by the time at which the sample is placed in the sample cell and is no longer subjected to any mechanical stress.

Figure 3 shows an example of the age dependence of the calculated auto-correlation functions $(g^{(2)}(Q,\tau,t_W)-1)$ at Q^* for different ages increasing from left to right. In the experiment we do not detect the β-relaxation of the translational dynamics which is too fast for our experimental set-up. We only probe the final α-process which is the final relaxation ($g^{(2)}(Q,\tau,t_W)-1$ tends to 0 at long times). The

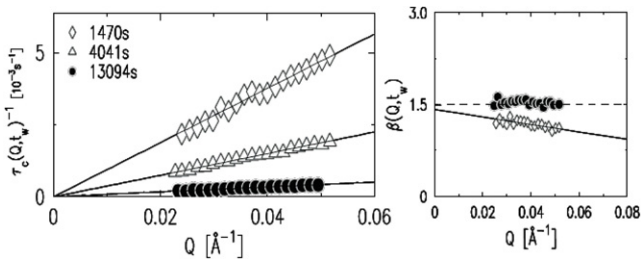

Figure 4. Left: Q dependence of the inverse characteristic relaxation time $\tau_C(Q,t_W)$ for three different ages: $t_W = 1470$, 4041 and 13 094 s. The solid lines are linear fits to the data. Right: Q and age dependence of the stretching exponent $\beta(Q,t_W)$, for ages 1470 and 13 094 s (same symbols as left panel). The solid line is a guide to the eye and the dashed line indicates 1.5 (error bars are smaller than symbols).

measured out-of-equilibrium translational dynamics capture on nanoscales generic features usually observed on microscales:

- a compressed exponential relaxation (see figure 3) such as

$$g^{(2)}(Q,\tau,t_W) - 1 \propto \exp\left(-2\left(\frac{\tau}{\tau_C(Q,t_W)}\right)^{\beta(Q,t_W)}\right) \quad (2)$$

  with $\beta(Q,t_W) > 1$,
- an age-dependent characteristic time $\tau_C(Q,t_W)$ scaling as Q^{-1} (see figure 4) evolving from exponential at young age to a slower behavior at large ages [6],
- no deviation from these behaviors observed in the vicinity of Q^* (which corresponds to the strongest spatial correlations) thus excluding local rearrangements at the scale of $2\pi/Q^*$ as the driving force for ageing in this system.

Such a ballistic-like relation of dispersion $\tau_C(Q,t_W)^{-1} \sim Q$ is frequently observed in attractive systems and rules out any cage-escape process for the present ageing behavior. It is frequently addressed as relaxation of randomly distributed stresses inside the system [3]. However, recent time resolved dynamic light scattering experiments performed on strongly attractive gels [12] have shown that such observations could

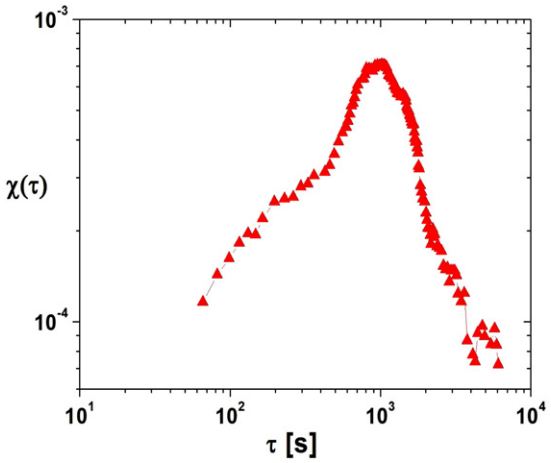

Figure 5. Normalized temporal variance $\chi(\tau)$ of c_I at Q^* as a function of the lag time τ.

be associated with series of rearrangement events that induce intermittent dynamics. These intermittent dynamics can be quantified by the dynamical susceptibility χ_4 introduced in simulations of glass formers, which corresponds to the volume integral of the four-point correlator [13–15].

We perform using the XPCS data the analysis of the dynamical fluctuations of the scattered patterns in terms of time resolved correlations [16]. The dynamics is observed to be also temporally heterogeneous and we quantify these heterogeneities following the method described in [17].

4. Time resolved correlation analysis—temporal heterogeneous dynamics

The instantaneous degree of correlation c_I between two different speckle patterns distant by a lag time τ can be computed along the elapsed time t as

$$c_I(Q,\tau,t) = \frac{\langle I_p(Q,t) I_p(Q,t+\tau)\rangle_Q}{\langle I_p(Q,t)\rangle_Q \langle I_p(Q,t+\tau)\rangle_Q} - 1 \qquad (3)$$

The average $\langle\cdots\rangle_Q$ is here defined as in equation (1). The intensity auto-correlation function $g^{(2)}(Q,\tau,t_W) - 1$ corresponds here to $\overline{c_I(Q,\tau,t)}$ where the overbar indicates the experimental time average over T_{exp} (associated with the definition of t_W in section 2). Even if the data are not shown, the c_I experimentally presents heterogeneous temporal fluctuations which are functions of both Q and τ. They are, as expected in a repulsive glass, of low amplitude.

A way to quantify these dynamical fluctuations is to calculate the normalized temporal variance $\chi(\tau)$ of c_I at fixed Q and τ [12, 17]. This quantity is analogous to the dynamical susceptibility χ_4 [13–15]. The calculation of the temporal variance of c_I is only possible in the regime of slow ageing, $t \geqslant 10^4$ s. Following the method detailed in [17], the data are corrected from the noise contribution due to the limited number of pixels of the CCD camera. An ageing correction is also realized by subtracting the mean slope of the time evolution of the c_I calculated for different lags τ. Despite the low temporal fluctuations, the dynamical susceptibility $\chi(\tau)$ of our repulsive glass is measurable. It is plotted in figure 5 as a function of τ for $Q = Q^*$, the calculation being performed for 10^4 s $< t <$ 3.10^4 s. It presents a peak at τ of the order of 10^3 s, which is of the same order of magnitude as the characteristic time τ_C obtained in section 2, at Q^* and for t_W of the order of a few 10^4 s. The maximum value of $\chi(\tau)$ is here much lower than the one measured for a strongly attractive gel [12], the fluctuations of the dynamics being less important in this repulsive glass.

5. Summary—perspectives

The dynamical susceptibility determination in a glass former consisting of spherical nanoparticles with repulsive interactions is here presented for the first time. The peaked shape of $\chi(\tau)$ is a strong experimental evidence of the intermittent nature of the dynamics, at the nanoscale. Such experimental determinations are still scarce and experimentally difficult to obtain. The heterogeneous character of the dynamics is expected to be a characteristic feature of all jammed systems and our results thus constitute an extension of its universality, to repulsive and nanometric glass formers.

We plan in the future to explore the Q and Φ dependence of the dynamical heterogeneities in dense magnetic fluids. The Q dependence of the dynamical heterogeneities for repulsive systems down to the nanoscale has until now been unknown. A modification of the fluctuations is expected [15] with an increase of the volume fraction of the dispersion. More precisely, a critical behavior of the dynamical susceptibility with the volume fraction could settle the jamming transition as a new class of dynamical phase transition. Last, the structure under an applied magnetic field of such a dense magnetic fluid is anisotropic and anisotropic ageing is also expected.

References

[1] Liu J and Nagel R 1998 *Nature* **396** 21–2
[2] Trappe V, Prasad V, Cipelletti L, Segre P N and Weitz D A 2001 *Nature* **411** 772–5
[3] Cipelletti L and Ramos L 2005 *J. Phys.: Condens. Matter* **17** R253–85
[4] Cousin F, Dubois E and Cabuil V 2003 *Phys. Rev.* E **68** 0214051–9
[5] Mériguet G, Dubois E, Dupuis V and Perzynski R 2006 *J. Phys.: Condens. Matter* **18** 10119–32
[6] Robert A, Wandersman E, Dubois E, Dupuis V and Perzynski R 2006 *Europhys. Lett.* **75** 764–70
[7] Mériguet G, Demouchy G, Dubois E, Perzynski R and Bourdon A 2007 *J. Non-Equilib. Thermodyn.* **32** 271–9
[8] Hasmonay E, Dubois E, Bacri J-C, Perzynski R, Raikher Yu L and Stepanov V 1998 *Eur. Phys. J.* B **5** 859–97
[9] Hasmonay E, Bee A, Bacri J-C and Perzynski R 1999 *J. Phys. Chem.* B **103** 6421–8
[10] Wandersman E, Dupuis V, Dubois E and Perzynski R 2008 at press
[11] Cipelletti L and Weitz D 1999 *Rev. Sci. Instrum.* **90** 3214
[12] Duri A and Cipelletti L 2006 *Europhys. Lett.* **76** 972–8
[13] Franz S and Parisi G 2000 *J. Phys.: Condens. Matter* **12** 6335

[14] Mayer P, Bissig H, Berthier L, Cipelletti L, Garrahan J-P, Sollich P and Trappe V 2004 *Phys. Rev. Lett.* **93** 115701
[15] Berthier L, Biroli G, Bouchaud J-P, Cipeletti L, El Masri D, L'Hôte D, Ladieu F and Pierno M 2005 *Science* **310** 1797–800
[16] Cipelletti L, Bissig H, Trappe V, Ballesta P and Mazoyer S 2003 *J. Phys.: Condens. Matter* **15** S257–62
[17] Duri A, Bissig H, Trappe V and Cipelleti L 2005 *Phys. Rev.* E **72** 051401